

## Interpreting atomic resolution EELS spectra using multiple scattering theory

Habib O. Moltaji, James P. Buban\* and Nigel D. Browning

Department of Physics (M/C 273), University of Illinois at Chicago, 845 West Taylor Street, Chicago, IL 60607-7059, USA. E-mail: [jbuban1@uic.edu](mailto:jbuban1@uic.edu)

By performing electron energy loss spectroscopy (EELS) in a scanning transmission electron microscope (STEM) it is possible to obtain atomic spatial resolution spectra from individual defects. Using the multiple scattering methodology originally developed for X-ray absorption Near-Edge Structure (XANES), the fine-structure of the energy loss spectra can be directly related to the local 3-dimensional atomic structure. This type of analysis allows unique structure models to be developed for defects, on which a fundamental understanding of the structure-property relationships can be based. The application of this technique is demonstrated here for a 25° [001] tilt grain boundary in SrTiO<sub>3</sub>.

**Keywords:** Multiple Scattering; EELS; Grain Boundaries.

### 1. Introduction

Grain boundaries and defects play a key role in controlling the structural and electronic properties of many oxide materials, such as ferroelectrics and high-T<sub>c</sub> superconductors. Typically such defects are analyzed by electron microscopy to provide images of the atomic structures (Pennycook and Jesson, 1990; Merkle and Smith, 1987). However, as these images are only 2-dimensional representations of the complete structure, and are relatively insensitive to oxygen and compositional fluctuations, analysis is limited to determining a set of probable defect structures. To proceed any further towards the ultimate goal of determining the local structure-property relationships, more information is needed. This information is provided by electron energy loss spectroscopy (EELS). Using a scanning transmission electron microscope (STEM) it has been demonstrated that spectra can be acquired with the same atomic resolution as the image (Browning *et al.*, 1993; Batson 1993; Duscher *et al.*, 1998).

The ability to obtain spectra at the same time and with the same atomic resolution as the images provides unique opportunities for the analysis of defects in oxide materials. In particular, as the energy loss spectrum is most sensitive to light elements while the image is most sensitive to the heavier cations, the use of the two techniques provides complementary compositional information. Furthermore, the energy loss spectrum gives detailed information on the local electronic structure at the defect and hence permits a direct correlation between the atomic structure and the electronic structure to be achieved. In order to attain this direct correlation, however, we need to develop a theoretical understanding of how the atomic structure affects the local electronic structure of the material. This is not straightforward in the case of defects, as the low-symmetry of the defect makes the use of complex *ab initio* simulation routines computationally prohibitive (Wu *et al.*, 1997).

One means to obtain the theoretical understanding of defects in oxides is through the use of multiple scattering (MS) analysis. The use of real space atomic clusters in MS analysis, makes it ideal for the analysis of the low-symmetry defect structures. In particular, the experimental image can be used as provide the basis of the cluster used in the simulations, thereby removing many of ambiguities that can be associated with modeling grain boundaries. The physics behind the excitation process in EELS is the same as that for X-ray absorption (the only change being the use of electrons instead of an X-ray to cause a particular excitation). This means that the codes originally developed for X-ray absorption Near-Edge Structure (XANES) can be used in this analysis (Durham *et al.*, 1981). In this case, however, we can acquire the spectra from specific atomic locations around a defect and use the analysis to develop a unique fundamental picture of both the atomic and electronic structure. In this paper we present one of our initial analysis of a 25° grain boundary in SrTiO<sub>3</sub>.

### 2. Multiple Scattering Theory

Multiple scattering calculations model the density of unoccupied states (as measured in the experimental spectrum) by considering the scattering of the photoelectron created during the excitation process, from neighboring atoms. The many paths which may be taken by a photoelectron, alter the matrix elements for a particular transition due to constructive or destructive interference, which occurs between the outgoing and returning photoelectron wave. Accurate and computationally efficient codes for the theoretical calculation of the multiple scattering paths have been developed by Rehr (1992) with the FEFF7 codes and by Binsted *et al.* (1992), with the EXCURE codes. These codes use the overlapping-atom prescription of Mattheiss (1964) to model the atomic potential within the muffin tin approximation. From the resulting potential, scattering phase shifts and matrix elements are calculated. The transition matrix elements of the absorption coefficient can be expressed in terms of the Green function in MS theory (Lee and Pendry, 1975). The Green function is expanded as a series corresponding to zero, single, double and higher order scattering, where zero order is scattering of the central atom and all other orders are scattering from the surrounding atoms. With this method, the total absorption coefficient  $\mu(E)$  can be represented by a contribution from the isolated atomic absorption  $\mu_0(E)$  with intensity modulations introduced through a structural factor  $\chi(E)$

$$\mu(E) = \mu_0(E) (1 + \chi(E))$$

$\chi(E)$  is the fractional change in absorption coefficient that is induced by neighboring atoms and can similarly be expressed as a sum of contributions corresponding to increasing numbers of scattering events

$$\chi(E) = \sum_{\Gamma} \chi_{\Gamma}(\rho),$$

where  $\chi(E)$  is the multiple scattering signal with the path  $\Gamma$  of order  $N$  ( $N > 1$ ). In the calculations presented here, core hole effects are included using the  $(Z+1)^*$  approximation (Brydson *et al.*, 1989), where  $*$  denotes the excited atom. For the purposes of these calculations, the atomic clusters are divided into shells of

atoms where a single shell is composed of atoms, which lie between two radii about the excited site. For SrTiO<sub>3</sub>, the calculations were found to converge for clusters including atoms up to the eighth shell, i.e.  $r=6.173 \text{ \AA}$  (Browning *et al.*, 1998).

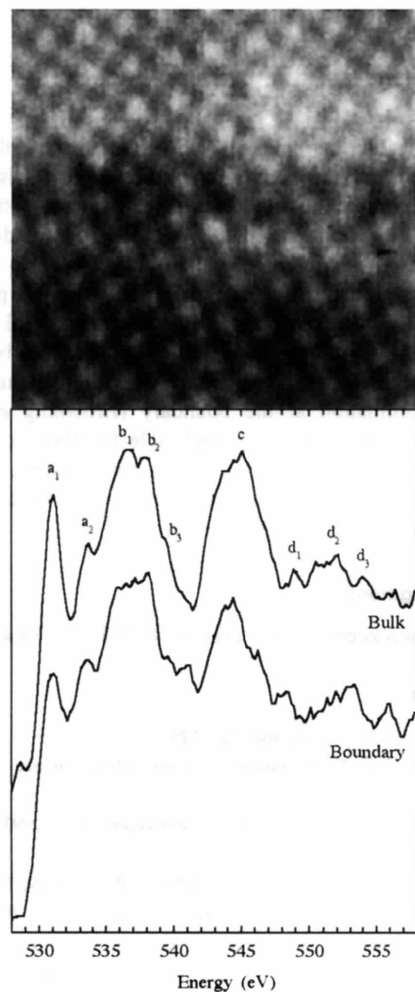


Figure 1: (a) Z-contrast image of the 25° [001] symmetric tilt grain boundary in SrTiO<sub>3</sub>. (b) Experimental Oxygen K-edge spectra from the bulk and boundary.

### 3. Experimental

The experimental Z-contrast image and energy loss spectra (Figure 1) were collected using a VG HB501 dedicated STEM operating at 100kV (2.2Å resolution) and equipped with a parallel detection EELS spectrometer (Browning *et al.*, 1993; McGibbon *et al.*, 1994). The energy resolution of the experimental spectra is ~0.8eV. The spectra are not deconvoluted to remove the effects of plural scattering (Egerton, 1996), so a direct comparison of peak intensities with the simulations will be subject to a systematic error. In this experiment, spectra were obtained at unit cell intervals across the boundary. However, for clarity only the bulk and boundary spectra are shown in figure 1. To avoid beam damage, the probe was scanned parallel to the boundary at each acquisition position, and hence, the spectrum contains the integrated signal from the entire boundary plane.

### 4. Analysis of the Spectra

Figure 2 shows the multiple scattering simulations for the bulk and the boundary obtained using the FEFF7 programs. To understand the effect that the boundary atomic structure has on the electronic structure and therefore the energy loss spectrum, it is first necessary to understand the fine-structure of the oxygen K-edge spectrum obtained from bulk SrTiO<sub>3</sub>. In analyzing the oxygen K-edge it is convenient to break to spectrum up into two sections. The first section, involving the first 5-10eV above the threshold, has been previously identified as resulting from hybridization between the oxygen 2*p* and transition-metal (Ti) 3*d* levels (Grunes *et al.*, 1982). As described by de Groot *et al.* (1993), the perovskite structure represents the prototype for a tight-binding description of the TiO<sub>6</sub><sup>8-</sup> cluster. Here, the crystal field splitting results in 2*t*<sub>2*g*</sub> states that are essentially pure π bonding and 3*e*<sub>g</sub> states that is pure σ bonding. The stronger σ interaction increases the dispersion of the *e*<sub>g</sub> band with the net result, which is reproduced in the experimental spectrum, that the *t*<sub>2*g*</sub> band (peak *a*<sub>1</sub>) appears more intense and narrower than the *e*<sub>g</sub> band (peak *a*<sub>2</sub>). In the MS spectra, the intensity and shape of peak *a*<sub>1</sub> is well reproduced, but peak *a*<sub>2</sub> is absent. The reason for its absence is rooted in the multiple scattering method used to simulate the spectrum. The muffin tin potentials used in the codes are spherically symmetric and therefore do not include the *d*-symmetry of the interaction between the oxygen 2*p* and titanium 3*d* orbital and are also not self-consistent.

This lack of self-consistency in the simulation routines is the main limitation to the analysis with the FEFF7 codes presented here. However, while it has been shown that self consistent Korringa-Kohn-Rostoker calculations (Rez *et al.*, 1998) and ab initio multiple scattering simulations (Wu *et al.*, 1997) can reproduce the crystal field splitting, the ability to apply these accurate methods to low-symmetry grain boundaries is not immediately obvious. As this is the first time that such detailed analysis of atomic resolution spectra from grain boundaries has been performed, the analysis presented here will focus on the trends observed in a comparison of experiment with experiment and theory with theory. This therefore assumes that the differences in intensities between the experiment and theory are a systematic error of the potentials used (given that most of the peaks are reproduced with approximately the correct intensity, this seems a valid first approximation). For this reason, as peak *a*<sub>1</sub> is reproduced in the FEFF7 calculations, the interpretation of the effect of the Ti nearest neighbors on the oxygen at the grain boundary will focus on this peak. The same caveat to the analysis and interpretation using the FEFF7 codes applies to the second part of the spectrum described below.

The second part of the spectrum concerns the range, 10-30eV above threshold. In this regime, band structure calculations show that oxygen 2*p* states are hybridized with the weakly structured metallic 4*sp* band (de Groot *et al.*, 1993). As such, the intensity modulations that occur in this energy range are not the result of transitions to bound states, but rather from interference effects resulting from multiple scattering of the excited photoelectron from neighboring atoms. As this is precisely the scattering that the FEFF7 codes are designed to calculate, it is not surprising that the theoretical spectrum reproduces these features with greater accuracy than the crystal field splitting. In particular, it has been

found that  $O^{2-}$  ions are strong backscatterers and the main peaks in the spectrum can be assigned to resonance effects between the excited atom and the oxygen cages (shells) that surround it (Kurata and Colliex, 1993). Using the resonance argument, the main peaks in the oxygen K-edge spectrum can be assigned to the following interactions; peak  $b_2$  results from intrashell scattering in the first shell of oxygen neighbors, peak  $c$  originates from single scattering from the shell containing the second nearest oxygen neighbors and peak  $d_2$  originates from single scattering from the shell containing the first nearest oxygen neighbors. The other peaks in the spectrum arisen either from multiple scattering events in higher shell ( $b_1$  and  $d_1$ ) or involve Sr atoms in the multiple scattering paths ( $b_3$  and  $d_3$ ).

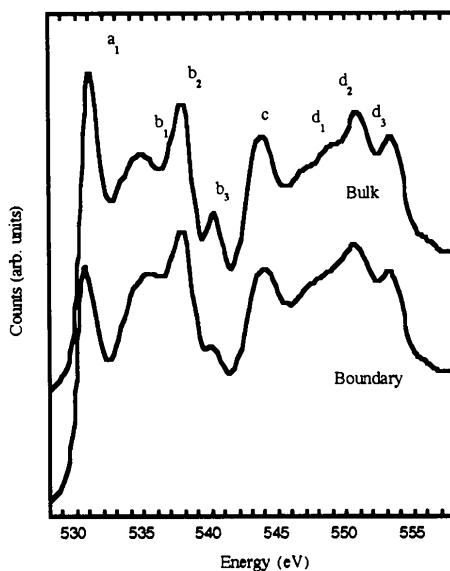


Figure 2: Multiple Scattering simulations of the bulk and boundary. The boundary clusters were determined from the structure observed in the image. In order to allow an accurate comparison between the experimental and calculated spectra, the energy scale of the calculations is modified using the function  $E_{EX} = C_0[\ln(E_{MS})]^2$ .

### 5. Interpreting the Boundary Structure-Property Relationship

With this analysis of the spectra in place, we are now in a position to interpret the spectral changes that occur at the grain boundary. In particular, peak  $a$  gives information on the coordination to the Ti nearest neighbors and peaks  $b_{1-3}$ ,  $c$  and  $d_{1-3}$  give an accurate and detailed analysis of the first and second nearest oxygen neighbors. By comparing the experimental spectra from the bulk and boundary, the main changes occurring at the boundary seem to be a decrease in peaks  $a_1$ ,  $b_1$ ,  $b_2$ ,  $c$  and  $d_2$ . A simple interpretation of this result suggests that atoms in the grain boundary plane have a reduced symmetry and reduced number of first and second nearest oxygen neighbors, i.e. a decrease in the backscattered intensity is caused simply by a decrease in the number of backscattering  $O^{2-}$  ions (Browning *et al*

*al*, 1998). From a simple ionic picture for  $SrTiO_3$ , this reduction in oxygen coordination effectively results in a positively charged boundary plane. Given the similarity of all [001] tilt boundary structures in  $SrTiO_3$  (Browning and Pennycook, 1996), this may be the origin of the widely observed electrical barriers at grain boundaries in  $SrTiO_3$  (Chiang and Takagi, 1990).

### 6. Conclusions

In conclusion, the present study demonstrates that multiple scattering analysis of electron energy loss spectra is a powerful tool to obtain direct correlation of EELS features with the atomic structure. This information can be used to provide a detailed three-dimensional structure for the grain boundary from which the structure-property relationships at the boundary plane can be elucidated. By considering the comparison EELS and MS calculation from bulk and boundary in  $SrTiO_3$  it has been possible to determine that there is an intrinsic structure induced reduced oxygen coordination at the boundary (Browning *et al*, 1998). These techniques are equally applicable to other oxide materials such as ferroelectrics and high- $T_c$  superconductors, and may be used to help elucidate a general atomic scale structure-property relationship for defects in these materials.

### Acknowledgment

Research sponsored by DOE grant # DE-FG02-96ER45610.

### References

- Batson, P. E. (1993) *Nature* 366, 727-729.
- Binsted, N., Srange, R., & Hasnain, S. (1992) *Biochemistry* 31, 12117-12125.
- Browning, N. D., Chisholm, M. F., & Pennycook, S. J. (1993) *Nature* 366, 143-146.
- Browning, N. D. & Pennycook, S. J. (1996) *J. Phys. D.* 29, 1779-1794.
- Browning, N. D., Moltaji, H. O., & Buban, J. (1998) *Phys. Rev. B.* 58, 8289-8300.
- Brydson, R., Sauer, H., Engel, W., Thomas, J. M. & Zeitler, E. (1989). *J. Chem. Soc. Chem. Commun.* 15, 1010-1017.
- Chiang, Y. M., & Takagi. T. (1990) *J. Am. Ceram. Soc.* 73, 3278-3285.
- de Groot, F. M. F., Faber, J., Michiels, J. J. M., Czyzyk, M. T., Abbate, M. & Fuggle, J. C. (1993). *Phys. Rev. B* 48, 2074-2079.
- Durham, P. J., Pendry, J. B., & Hodges, C. H. (1981) *Solid State Commun.* 38, 159-162.
- Duscher, G., Browning, N. D., & Pennycook, S. J. (1998) *Phys. Stat. Sol. A.* 166, 327-342.
- Grunes, L. A., Leapman, R. D., Wilker, C. N., Hoffman, R. & Kunz, A. B. (1982). *Phys Rev B* 25, 7127-7131.
- Kurata, H. & Colliex, C. (1993). *Phys. Rev. B* 48, 2102-2108.
- Lee, P. A., & Pendry, J. B. (1975) *Phys. Rev. B.* 11, 2795-2800.
- Mattheiss, L. (1964). *Phys. Rev. A* 133, 1399-1403.
- McGibbon, M. M., Browning, N. D., Chisholm, M. F., McGibbon, A. J., Pennycook, S. J., Ravikumar, V., and Draavid, V. P. (1994). *Science* 266, 102-104.
- Merkle, K. L. & Smith, D. J. (1987). *Phys. Rev. Lett* 59, 2887-2890.
- Pennycook, S. J. & Jesson, D. E. (1990). *Phys. Rev. Lett* 64, 938-941.
- Rehr, J. J., Albers, R. C., & Zabinsky, S. I. (1992). *Phys. Rev. Lett* 69, 3397-3400.
- Rez, P., MacLaren, J. M., & Saldin, D. K. (1998) *Phys. Rev. B.* 57, 2621-2630.

(Received 10 August 1998; accepted 7 December 1998)